

Grain-boundary theory of melting in two dimensions

S. T. Chui

Bartol Research Foundation of the Franklin Institute, University of Delaware, Newark, Delaware 19711

(Received 1 September 1982)

A theory of melting in two dimensions via the spontaneous generation of grain boundaries is worked out. We find that this mechanism is more favorable than the dislocation unbinding mechanism and that a first-order phase transition always results. The transition goes from strongly first order to weakly first order for a core energy E_B less than $2.84kT_0$ (T_0 being the temperature at which the dislocations unbind), consistent with recent estimates by Saito. The question of the hexatic phase is discussed.

I. INTRODUCTION

Melting in two dimensions has been a subject of interest recently. Many computer simulations¹ for different interparticle potentials have been done, but the results do not fit in well with the calculations using the dislocation unbinding mechanism (DUM) by Kosterlitz and Thouless² and by Halperin and Nelson.³ All computer simulations show a dramatic increase in the total number of dislocations as the system goes into the liquid phase, whereas the DUM predicts no change in the total number of dislocations. Also, the DUM predicts a gradual increase in the separation of some of the dislocation pairs, but this is not seen. Some computer simulations indicate a first-order phase transition, whereas the DUM produces a continuous phase transition. The possible effects of dislocations in melting has been discussed in the past by Mizushima, Kuhlmann-Wilsdorf, Nabarro, Cotterill *et al.*, and more recently by Edward and Warner.⁴ An alternative mechanism of melting via the spontaneous generation of grain boundaries was discussed thirty years ago,⁴ but no detailed calculation was carried out. Recently Fisher, Halperin, and Morf⁵ pointed out that the free energy to generate a single small-angle grain boundary goes to zero at the temperature T_0 where the dislocations unbind. We have studied the statistical mechanics of a collection of grain boundaries on a hexagonal lattice and find the following features: (a) Grain boundaries are generated before T_0 as the temperature is increased; (b) when coupled either to a finite density change or to bound dislocation pairs a first-order phase transition always results; (c) the transition goes from strongly first order to weakly first order for a core energy less than $2.84T_0$; (d) a hexatic phase will not exist for $T > T_0$. Since a grain boundary consists of an array of dislocations,⁶ spontaneous generation of grain boundaries implies a dramatic increase in the total number of disloca-

tions, a result more consistent with computer simulations.

We have looked at three different possible configurations of grain boundaries illustrated in Fig. 1 and have found that Fig. 1(b) is most favorable. Our results are summarized by the expansion for the free energy F_i of these different configurations in terms of the density of the grain boundaries n (of one orientation but including the two directions of the

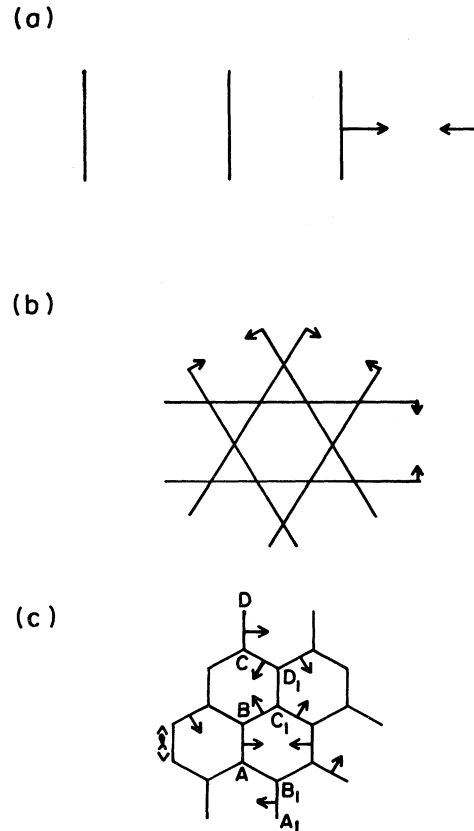


FIG. 1. Three possible arrangements of the grain boundaries. (b) is the most favorable.

Burgers vector):

$$F_i = -A_i(T - T_i)n + B_i n^2 + C_i/n + D_i n^3 + O(n^4). \quad (1)$$

The coefficients are given in Eqs. (6) and (22). But let us describe our results briefly here.

The coefficient of the term linear in n comes from considerations of the free energy of an isolated grain boundary and its interaction with bound dislocation pairs. C_1, C_2 are equal to zero but C_3 is positive. Hence the configuration in Fig. 1(c) is highly unfavorable. There are two sources that all contribute to a negative n^2 term. They come from (i) a grain-boundary crossing energy and (ii) a density change coupling energy. The first source applied to Fig. 1(b) only. Because of this negative n^2 term we expect a first-order phase transition to occur near T_i ($=T_0$), the Kosterlitz-Thouless transition temperature.

Our calculation is based on linear-elasticity theory. We first calculate the energy of the configurations in Fig. 1 at zero temperature. This is discussed in Sec. II. In Sec. III we investigate finite temperature effects by considering small deviations from these configurations. The grain-boundary crossing energy, the coupling to the density change, and to bound dislocation pairs are discussed in Sec. IV. The shear modulus of the grain-boundary network is discussed in Sec. V. One difference between grain-boundary theories of melting in two and three dimensions is pointed out. In Sec. VI we conclude by discussing the question of the hexatic phase. A discussion of the physical origin of the various terms in Eq. (1) can be found in Ref. 7. A summary of our results can be found in Ref. 8. Both these publications contain numerical errors which have been corrected in this paper.

II. ZERO-TEMPERATURE RESULTS

In this paper we shall assume that grain boundaries are just arrays of dislocations with density s^{-1} chosen to optimize the free energy. Elastic energies of grain boundaries can be obtained by summing the contributions from individual dislocations. The details of calculations in this section are discussed in Appendix A. The only assumptions in this calculation are that of linear-elasticity theory.

Dislocations with Burgers vectors \vec{b}, \vec{b}' interact with each other with a potential of the form

$$V = \frac{-K}{4\pi} \left[k_1 \ln |\vec{r} - \vec{r}'| \vec{b} \cdot \vec{b}' - k_2 \frac{\vec{b}' \cdot (\vec{r} - \vec{r}') \vec{b} \cdot (\vec{r} - \vec{r}')}{|\vec{r} - \vec{r}'|^2} \right], \quad (2)$$

where K is a function of the elastic constants. In the absence of an external orientational field $k_1 = k_2 = 1$.

From this, one can calculate the energy U of two parallel arrays of dislocations (grain boundaries) with opposite Burgers vectors a distance z apart as [see Fig. 2(a)] $U(r) = \sum_i V(r - r_i)$. If only the first term in (2) was present from potential theory U would be proportional to only z . Then it would be impossible to take the two grain boundaries apart. When the second term is included, the long-range interaction is canceled out and one ends up with a short-range potential of the form⁶ [see Appendix A(1)]

$$U(z, K) = \frac{L}{s} \frac{K}{4\pi} \left[\ln \sinh \left[\frac{\pi z}{s} \right] - \frac{\pi z}{s} \coth \left[\frac{\pi z}{s} \right] + \ln \left[\frac{s}{\pi} \right] \right] = \frac{L}{s} \tilde{U}. \quad (3)$$

This cancellation is complete only for an infinite array of dislocations. For this reason finite arrays of dislocations are ignored. Note that in the DUM, the

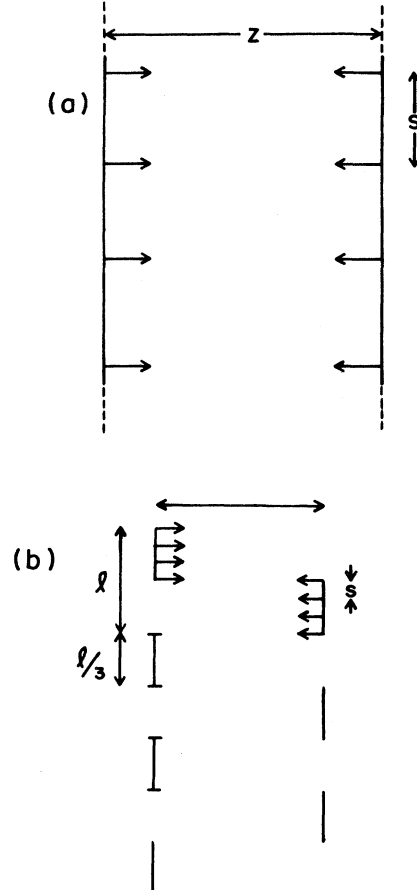


FIG. 2. Two simple building blocks for grain-boundary networks. s is the interdislocation spacing.

second term in (2) is much less significant compared with the first term, and it is much more difficult to take the dislocations apart. Thus in the grain-boundary mechanism there is a special correlation of the direction of all the Burgers vectors that is built in. In the DUM, one can only include the correlations of the directions of *two* Burgers vectors; hence the effective interaction still remains long ranged.

From Eq. (3) the energy at $T=0$ of configurations 1(a) and 1(b) can be computed. A key simplification comes from the cancellation of the average interaction of nonparallel grain boundaries if the correlation of the positions of the dislocations of the intersecting grain boundaries is ignored. This correlation is important and is discussed in Sec. IV. As $z \rightarrow \infty$,

$$\tilde{U} \rightarrow (K/4\pi) \ln(s/2\pi).$$

Hence the zero-temperature energies E_1, E_2 for con-

$$\begin{aligned} W(z) &\rightarrow \frac{K}{16\pi^3} \sum_{m>0} \frac{l^2}{s^2} \left[\frac{1}{m} + \cos(\pi m) \exp[-\sqrt{3}\pi m (\pi\sqrt{3}-1)] \right] \frac{\sin^2(\pi m/3)}{m^2} \\ &\cong \frac{K}{16\pi^3} \sum_{m>0} \frac{l^2 \sin^2(\pi m/3)}{s^2 m^3}. \end{aligned} \quad (5)$$

From this we get

$$C_3 = \frac{3}{l^2} W(0.866l) \cong \frac{9K}{64\pi^2 s^2}, \quad (6)$$

$$C_2 = C_1 = 0.$$

As we emphasized in Sec. I, this implies that Fig. 1(c) is highly unfavorable and it will be ignored from now on.

In all the above calculations we have assumed that the Burgers vectors are perpendicular to the grain boundary (Fig. 3). In Appendix A(3) we have also

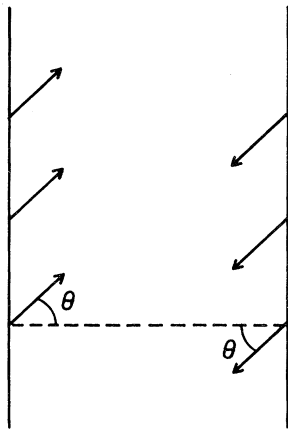


FIG. 3. Tilted grain boundaries.

figurations 1(a) and 1(b) are

$$E_1 = \frac{K}{8\pi} \frac{n}{s} \ln \left[\frac{s}{2\pi} \right] \quad (4a)$$

and

$$E_2 = 3E_1 \quad (4b)$$

The energy of configuration 2(c) can be computed from the energy W of the pair $ABCD, \dots, A_1B_1C_1D_1, \dots$ illustrated in Fig. 1(c) and more clearly in Fig. 2(b) [see Appendix A(2)]. Again the average grain-boundary crossing energy cancels. (The calculation is facilitated by expanding the dislocation density as a Fourier series.) We find, for $z/s \rightarrow \infty$ that $W(z)$ is dominated by interactions between dislocations on the "same" grain boundary (such as $ABCD, \dots$):

calculated the energy of configurations with the Burger vector not perpendicular to the grain boundary and found them to be energetically unfavorable.

III. FINITE-TEMPERATURE RESULTS

Here we discuss finite-temperature results by considering small deviations from the zero-temperature configurations. There are three contributions to this: (a) that from an isolated boundary, (b) that from interactions between parallel boundaries, and (c) that from boundary crossings. (c) will be considered in the next section.

Let us consider (a) first. In the previous section, we have assumed that the positions of the dislocations are periodically arranged at r_i^0 . Now let $r_i = r_i^0 + \delta r_i$, and expand Eq. (2a) as

$$\begin{aligned} U &\cong \sum V(r_i^0 - r_j^0) + \frac{1}{2} \sum (\delta r_i^0 - \delta r_j^0)^2 V'' \\ &= U(z, K) + Y. \end{aligned}$$

$U(z, K)$ is defined in Eq. (3). Y is an energy functional of distortion of the form [see Appendix A(4)]

$$Y = \sum_i (\gamma |q| + \Delta) |\delta \vec{r}_{iq}|^2. \quad (7)$$

Here $\delta \vec{r}_{iq}$ is the Fourier transform of the configuration of the i th grain boundary. γ is given by

$$\gamma = b^2 K / 8s . \quad (8)$$

Δ is significant only if the grain boundaries are close together. For two grain boundaries at a distance z from each other,

$$\Delta = (b^2 K \pi / 4s^2) \text{csch}^2(\pi z / s)$$

for longitudinal modes. For transverse modes potential (3) provides a short-range term linear in δr_{iq} .

When the grain boundaries are far apart so that Δ is negligible one gets by integrating the Boltzmann factor $\exp(-\beta Y)$ over all possible configurations $\delta \vec{r}_{iq}$ the finite-temperature contribution to the free energy G_2 of noninteracting grain boundaries [see Appendix B(1)], viz.

$$G_2 \cong -(3Tn/s)[2 \ln s + 1 + \ln(T/2\pi T_0)] . \quad (9)$$

When the grain boundaries are close together part of this free energy is lost.

Let us next discuss the interaction free energy between "parallel" grain boundaries. Because of the thermal fluctuation, two grain boundaries can come close together at certain places. Whenever this happens because of the hard-core repulsion between parallel grain boundaries, some entropy is lost. If the elastic energy Y were proportional to q^2 then this "entanglement" energy is of the order of n^3 .⁹ Now the grain boundary is stiffer so that the chances of entanglement and hence the loss in entropy is reduced. Estimates in Appendix B(2) indicate that it is of the order of $n \exp(-\text{const}/Tn^2)$. For small n this term is much smaller than the terms in Eq. (1). Hence it is neglected.

IV. GRAIN BOUNDARY CROSSING ENERGY, COUPLING TO A DENSITY CHANGE AND BOUND DISLOCATION PAIRS

Here we discuss three other sources which contribute to the free energy. These include (1) an energy due to correlations of dislocations on crossing grain boundaries, (2) an energy due to the interactions of grain boundaries and bound dislocation pairs, and (3) an energy due to the coupling with the density change. We now discuss them in detail.

(1) *Grain-boundary crossing energy.* First let us say a few words about the basic physics involved. The dislocations inside a grain boundary can move. When two grain boundaries cross their dislocations stay closer together (further apart) if they attract (repel) each other. Even though a single grain boundary crosses equal numbers of dislocations of opposite Burgers vectors, because of this correlation, there is a net energy gained.

The dislocations inside a grain boundary are, however, coupled elastically. As a dislocation is at-

tracted by that of another grain boundary, another dislocation on the same boundary is also affected through this elastic coupling. Now we first estimated the energy by ignoring this coupling. Its effect will be estimated in the next paragraph. The calculation is reduced to that involving two essentially free dislocations. For $T \simeq T_0$, we get the following contribution to the free energy [see Appendix B(3)]:

$$H_1 = -n^2 T \epsilon(s) , \quad (10)$$

$$\epsilon(s) = \frac{1}{2} [\ln s + \ln(\pi \sqrt{3}/2)] , \quad (11)$$

$$H_2 = 3H_1 .$$

Note that for large s , $\epsilon(s) \rightarrow \ln s$.

We now estimate the elastic energy expanded to achieve the above gain. The force range between the grain boundaries is of the order of s/π . The average displacement δr_{iq} of a dislocation is thus of the order of $s/2\pi$. The average wave vector q of the strain is of the order of n . Using Eq. (7) the average strain energy is of the order of

$$N_2 N_1 \gamma (s/2\pi)^2 n . \quad (12)$$

Here $N_1 = L/s$ is the total number of dislocations on a grain boundary, $N_2 = Ln$ is the total number of dislocations. Hence we get an energy of the order of

$$L^2 n^2 K / 32\pi^2 . \quad (13)$$

Note that this term is always less than that in (10) for a large enough s , since the former is of the order of $\ln s$.

This can be combined with (12) and we get a

$$\bar{\epsilon}(s) = \epsilon(s) + 1/2\pi . \quad (14)$$

Some free energy is lost when three grain boundaries of different orientations are all close together. The probability of this occurring is of the order of $(2sn/\pi)$. In that case there is effective screening between dislocations, and it is not possible to gain the free energy $T_0 \epsilon(s)$ that we just calculated. We expect that H_1 should be modified to read

$$\begin{aligned} \bar{H}_1 &= H_1 + n^2 \bar{\epsilon}(s) T (2sn/\pi) , \\ \bar{H}_2 &= 3\bar{H}_1 . \end{aligned} \quad (15)$$

(2) *Coupling with bound dislocation pairs.* There is always a finite density of bound dislocation pairs present at temperatures below the Kosterlitz-Thouless transition. When grain boundaries are created they will interact with these dislocation pairs. We show here that this coupling induces an additional negative term in the free energy for the grain boundaries. We assume the low-density limit for both the dislocations and grain boundaries, and consider the interaction between a dislocation pair

and a parallel rigid grain boundary. The free energy \tilde{F} is given approximately by

$$e^{-\beta\tilde{F}} = \int d\vec{r} d\vec{r}' \exp\{-\beta[(K/4\pi)\ln|r-r'| - \tilde{U}(r) + \tilde{U}(r') + 2E_c]\}, \quad (16)$$

where \tilde{U} is the interaction between a dislocation and a grain boundary [Eq. (A13)].

In the absence of the grain boundary, the free en-

$$e^{-\beta(\tilde{F}-\tilde{F}_0)} = \frac{\int d\vec{r} d\vec{r}' |r-r'|^{-4} \exp\{-\beta[\tilde{U}(r') - \tilde{U}(r)]\}}{\int d\vec{r} d\vec{r}' |r-r'|^{-4}}. \quad (17)$$

This is evaluated approximately in Appendix C. One obtains finally that the interaction energy between the grain boundaries and the dislocation pair per unit area is given by (Appendix C)

$$\begin{aligned} \Delta F/n &= \tilde{F} \exp(-\beta\tilde{F}) - \tilde{F}_0 \exp(-\beta\tilde{F}_0), \\ \tilde{F} - \tilde{F}_0 &\cong -T \ln[1 - ns^{-1} + ns^2/12 \\ &\quad - n^3 s^4(1-s^3)/3], \\ \tilde{F}_0 &= 2E_c - T \ln[\pi/(2T/T_{KT} - 1)]. \end{aligned} \quad (18)$$

Note that if ns^3 is less than one then $\tilde{F} - \tilde{F}_0 \propto ns^3$ and we get a term linear in n .

(3) *Coupling with the density change.* Most melting transitions are accompanied by a finite-density change $\Delta\rho$. This change can easily be incorporated phenomenologically by including in F the following terms:

$$F' = \frac{(\Delta\rho)^2}{\rho} \frac{1}{2\kappa} + \lambda \frac{\Delta\rho}{\rho} \frac{n}{s}. \quad (19)$$

Here κ is the compressibility of the system, and λ comes from anharmonic strain effects. It is straightforward to minimize F' with respect to $\Delta\rho/\rho$. One gets an additional negative term in n^2 , viz.

$$F'_{\min} = \frac{-(\lambda n/s)^2}{2} \frac{1}{\kappa}. \quad (20)$$

Thus the coupling to strain is to make the transition more first order. In some cases such as the $1/r$ potential,⁸ κ is infinite (provided the boundary condition is right). Then this contribution vanishes.

V. THE SHEAR MODULUS

So far we have implicitly assumed that as the grain boundaries are created, the shear modulus in the new phase will be zero. In this section it will be demonstrated.

The dislocations along the grain boundary are specified by the set of coordinates $\{x_i\}$. The shear

energy F_0 of the dislocation pair is given by

$$e^{-\beta\tilde{F}_0} = \int dr dr' \exp[-\beta(K/4\pi)\ln|r-r'|] \times e^{-2\beta E_c}.$$

Close to T_0 , the change in free energy per pair is hence given by

modulus is related to the response function of the dislocations along the chain. More precisely, if one can move the dislocations along the grain boundary with zero energy barrier then the shear modulus is equal to zero. The potential energy of the dislocations consist of two parts. First, there is the elastic energy of the form

$$H_1 = \gamma \sum_q |q| |x_q|^2$$

that we discussed in Sec. III. Second, due to the atomistic nature of the system there is the Peierls-type potential

$$H_2 = \lambda \sum_i \cos(2\pi x_i).$$

This term has been left out in our discussions so far. This Peierls potential provides an activation barrier and renders the problem less trivial. By a duality-type transformation, as is done in the context of the roughening transition, the partition function

$$\int \prod_i dx_i \exp[-\beta(H_1 + H_2)]$$

can be mapped into that of a collection of one-dimensional (1D) Coulomb rods and hence into the Kondo problem. (See Appendix D.)

In that case we find that the shear modulus is zero for $T \geq T_0/8$ in the limit of small λ . Hence we expect the shear modulus to be zero at melting. This also implies that polycrystalline material may be unstable above a finite temperature.

VI. CONCLUSION

Let us summarize our findings here. The free energy F_2 can be written as

$$F = -A_i(T - T_i)n + B_i n^2 + C_i/n + D_i n^3 + O(n^4) + \Delta F_i. \quad (21)$$

From Eqs. (20), (18), (15), (14), (10), and (4), we obtain, for T close to T_0 , the following results:

$$\begin{aligned}
A_1 &= \frac{2 \ln s}{s}, \quad A_2 = 3A_1, \\
T_i &= \frac{K}{16\pi} + \frac{1}{2} \left[E_c - 2.84 \frac{K}{16\pi} \right] \frac{1}{\ln s}, \\
B_1 &= 0, \quad B_2 = -3T_0 \bar{\epsilon}(s) - \frac{1}{2} \kappa (\lambda n / s)^2, \\
C_1 &= C_2 = 0, \quad C_3 > 0, \\
D_1 &= T_s \frac{2\bar{\epsilon}(s)}{\pi}, \quad D_2 = 3D_1, \\
\Delta F_1 &= \Delta F_2 = 3 \Delta F_1.
\end{aligned} \tag{22}$$

ΔF arises from the interaction between bound dislocation pairs (of density σ) and grain boundaries.

Note that a negative grain-boundary crossing energy favors the configuration in Fig. 1(b). We shall focus on this from now on. There are two contributions to the n^2 term, both giving a negative contribution. They come from a grain-boundary crossing energy and a coupling energy with the density change. Because of these negative n^2 terms, we expect the transition to be first order. There may be situations such that the coupling with the elastic strain is absent. (For example, when the system is incompressible, such as for the $1/r$ potential,¹⁰ or certain situations in the Gaussian core potential.¹¹) In the absence of the coupling to the elastic strain the physics is quite subtle; the grain-boundary crossing energy by itself may be insufficient to generate a first-order transition. Instead, it is the combination of this term and ΔF which always generates a first-order transition. More explicitly, for $\kappa=0$, F_2 can be written as (in the limit of large s):

$$\begin{aligned}
F_2 &= -\frac{n}{2} \left\{ \ln s \left[-6(T - T_0) - T_0 \frac{ns}{2} \left(1 - \frac{2ns}{\pi} \right) \right] \right. \\
&\quad \left. + (E_c - 2.84T_0) \right\} + 3 \Delta F.
\end{aligned}$$

We have explicitly collected those terms proportional to $\ln s$. First let us assume that ΔF was absent. Note that both n and s are adjustable parameters. If $E_c - 2.84T_0$ is less than zero then F_2 becomes negative at a temperature before T_0 with a finite change of n and s . If $E_c - 2.84T_0$ is positive, however, the free energy is minimized if the $\ln s$ terms dominate. In that case we expect a transition to occur at a temperature T_1 given by

$$T_1 = T_0(1 - \pi/96),$$

corresponding to $ns \simeq \pi/4$. (T_1 represents the minimum reduction of the transition temperature with respect to T_0 , irrespective of the sign of $E_c - 2.84T_0$.) In this limit only the product ns as-

sumes a finite value when the phase transition occurs but s would like to be as large as possible and we expect the transition to be continuous.

When ΔF is incorporated then the above ‘‘accident’’ does not happen anymore. Note that the $\ln s$ term in F_2 depends actually on $(n \ln s)/s$ whereas ΔF has the functional form $\ln(1 + ns^3)$. Hence we expect the transition to be always first order. However, the transition is much more weakly first order for $E_c > 2.84T_0$. This is consistent with a recent Monte Carlo simulation of the vector Coulomb gas by Saito¹² who found a rapid change in the degree of discontinuity at a core energy in between $3.28T_0$ and $2.3T_0$. For compressible systems, as we pointed out in Sec. IV(3), the coupling to a finite density change induces a change in the core energy. Hence for systems interacting with a r^{-n} potential with $n > 1$, we expect a more favorable situation for the above mechanism. For r^{-1} potentials, no such reduction is possible. Estimates indicate⁵ that $E_c \simeq 4.9T_0$. We thus expect the transition to be more weakly first order in that case.

Because of the linear coupling to the bound dislocation pairs, we expect that as the grain boundaries appear there will also be a discontinuous change of the density of the bound dislocation pairs as well. It is difficult at the moment to give a precise estimate of the actual transition temperature. A crude guide is given by T_1 , which provides for a reduction of at least 1% relative to the Kosterlitz-Thouless temperature. This is certainly consistent with computer simulations with $1/r^n$ potentials ($n=12$ to $n=1$) which, with an uncertainty of about 10%, predicts a transition temperature in agreement with the Kosterlitz-Thouless temperature.

Let us next turn our attention to the so-called hexatic phase. In two dimensions, even though there is no positional long-range order, there can still be bond-orientational long-range order. This was first pointed out by Mermin.¹¹ Halperin and Nelson³ pointed out that in the DUM after the dislocations unbind the bond-orientational order exhibit power-law decay. This phase is called the hexatic phase. They suggested that there exists another transition at which this bond-orientational algebraic order is lost. We now investigate the bond-orientational order in the context of grain boundaries. In order for such a possibility to occur, it is necessary to have power-law correlation or some other long-range correlation for the orientational order parameter $e^{6i\theta}$. The orientation of a crystal changes as one goes from one side of a grain boundary to another. The direction of rotation is related to the ‘‘sign’’ of the Burgers vector of the grain boundary. It is obvious that the mean-square fluctuation of θ is proportional to the mean-square fluctuation of θ is proportional to the mean-square fluctuation of θ .

tuation of the net sum of the Burgers vector of the grain boundaries. If the grain boundaries with opposite Burgers vectors form bound states, then there is long-range correlation in θ . This is because if one crosses a grain boundary and the orientation of the crystal is rotated, one always encounters a grain boundary with opposite Burgers vectors and the orientation is restored. If bound states are not formed then

$$\langle \phi(0)\phi(R) \rangle \propto R$$

and

$$\langle e^{6i\phi(0)} e^{6i\phi(R)} \rangle \propto e^{-R\alpha}$$

where α is some constant of proportionality; the hexatic phase will then not exist.

To determine the possibility of a bound state it is necessary to know the effective attractive potential between the boundaries. In addition to the potential in Eq. (3), there is an additional term of the following origin. Whenever z/s is small, Δ in Eq. (7) for the longitudinal modes is no longer negligible. The entropy of the grain boundary is hence reduced. The resultant effective potential (see Appendix E) is the difference between Eq. (3) and the loss in entropy due to the gap. For small z , it is

$$U_{\text{eff}} = s^{-1}(4T_0 - 2T)\ln(\pi z/s) + 0.466T_0/s.$$

For $z > s/\pi$, U_{eff} approaches zero exponentially fast. Using U_{eff} , one can estimate the net gain in free energy for any part of the grain boundary that is closer than s/π . This turned out to be

$$-(4T_0 - 4T)\ln s + 3.6T_0.$$

Hence for $\ln s \leq 0.9(T_0 - T)$ no bound state can form.

Heiney *et al.*¹⁰ recently found that for xenon on graphite the transition becomes second order for coverages larger than 1.1 monolayers. This may be due to a change in the core energy. While graphite is incommensurate with xenon, it does impose an orientational ordering field on the epitaxy. The effect of this we have not fully investigated here. An indication of what will happen can, however, be glimpsed by the following argument. The potential $V(r)$ between two dislocations of Burgers vectors b, b' is given by

$$V(r) = -\frac{K_1}{8\pi} \vec{b} \cdot \vec{b}' \ln r + \frac{K_2}{8\pi} \frac{\vec{b} \cdot (\vec{r} - \vec{r}') \vec{b}' \cdot (\vec{r} - \vec{r}')}{|\vec{r} - \vec{r}'|^2}.$$

In the presence (absence) of an external orientational field $K_1 \neq K_2$ ($K_1 = K_2$). The potential between

grain boundaries is obtained by summing over the potential of the dislocations that make up the grain boundary. For $K_1 = K_2$ there is a cancellation between the first and the second term of V so that the potential between grain boundaries become short ranged. In the presence of an external orientational field $K_1 \neq K_2$, the cancellation is incomplete, the grain boundaries are always bound so that there is always orientational order, a result not too unexpected since now we have an external orientational field. However, it is not clear now whether the grain-boundary mechanism or the dislocation-unbinding mechanism is more important. It is conceivable that for a sufficiently large external field, the DUM takes over and the transition then becomes second order again.

In this paper we have demonstrated that the grain-boundary mechanism (GBM) is more favorable than the DUM. The GBM also fits in better with computer simulation results in that a dramatic increase in the total number of dislocations is predicted. We have not considered the interaction of grain boundaries with other point defects such as interstitials or vacancies. Nor can we rule out other possible mechanisms. There are certain predictions of the present theory which one should be able to compare with computer simulations. These include the dependence of the melting temperature on the core energy E_c , as well as the coupling to the density change.

ACKNOWLEDGMENTS

I thank J. D. Weeks and J. M. Kosterlitz for helpful conversations. This work was begun while the author was a summer visitor at Bell Telephone Laboratories; the support received there is appreciated.

APPENDIX A

Here the elastic energy of different configurations of grain boundaries is calculated. We take the model such that grain boundary is just an array of dislocations. Dislocations with Burger vectors \vec{b}, \vec{b}' interact with each other with a potential of the form

$$V = V_1 - V_2, \\ V_1 = \frac{K}{4\pi} \vec{b} \cdot \vec{b}', \ln |\vec{r} - \vec{r}'|, \\ V_2 = \frac{K}{4\pi} \frac{\vec{b} \cdot (\vec{r} - \vec{r}') \vec{b}' \cdot (\vec{r} - \vec{r}')}{|\vec{r} - \vec{r}'|^2}.$$
(A1)

K is given in terms of the Lamé constants λ, μ by

$$K = 4a^2 \frac{\mu(\mu + \lambda)}{(2\mu + \lambda)}.$$
(A2)

a here is the lattice constant and is set equal to 1 in

this paper.

(1) Let us first consider the energy E_a of the configuration in Fig. 2(a). This was first calculated by Reed and Shockly.⁶ Our calculation differs slightly from theirs in that we focus on the potential energy. It can be easily carried out with the following mathematical identities:

$$\sum_{\substack{n=-\infty \\ (n \neq 0)}}^{+\infty} \ln \left[\frac{n^2 + u^2}{n^2} \right] = 2[\ln \sinh(\pi u) - \ln(\pi u)], \quad (\text{A3})$$

$$\sum_{n=-\infty}^{\infty} \frac{1}{n^2 + a^2} = \frac{\pi}{a} \coth(\pi a). \quad (\text{A4})$$

E_a is just given by

$$E_a = + \frac{K}{8\pi} \left[\sum_n \ln(z^2 + n^2 s^2) - 2 \sum_n \frac{z^2}{z^2 + n^2 s^2} \right]. \quad (\text{A5})$$

Using (A3) and (A4) we thus get

$$E_a = + \frac{K}{8\pi} \left[\ln \sinh \left[\frac{\pi z}{s} \right] - \pi \frac{z}{s} \coth \left[\frac{\pi z}{s} \right] - \ln \pi + \ln s \right]. \quad (\text{A6})$$

Two special limits are worth recording.

(a) As $z/s \rightarrow \infty$

$$E_a \rightarrow + \frac{K}{4\pi} \left[\ln \frac{s}{2\pi} - 2 \frac{\pi z}{s} e^{-2\pi z/s} \right]. \quad (\text{A7})$$

(b) As $z/s \rightarrow 0$

$$E_a \rightarrow + \frac{K}{4\pi} (\ln z - 1). \quad (\text{A8})$$

$$E'_a = + \frac{K}{8\pi} \left[\ln[\cosh(2\pi z) - \cos(2\pi b)] - \ln(2\pi^2) + 2 \ln s - 2\pi z \frac{\tanh(\pi z)}{1 + \tan^2(\pi b)} [\tan^2(\pi b) + \tanh^2(\pi z)] \right]. \quad (\text{A11})$$

Note that as $z \rightarrow \infty$,

$$E'_a \rightarrow + (K/4\pi) \ln(s/2\pi). \quad (\text{A12})$$

As $z \rightarrow 0$,

$$E'_a \rightarrow \frac{K}{8\pi} \ln(z^2 + b^2) - \frac{K}{4\pi} \frac{z^2}{z^2 + b^2}. \quad (\text{A13})$$

For $b=0$ formula (A6) is recovered.

(3) One might also be interested in a configuration in which the direction of the Burgers vector is not

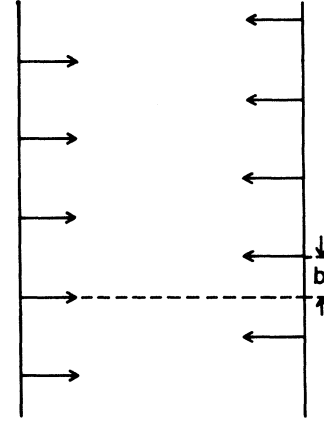


FIG. 4. Displaced grain boundaries.

(2) We record here some further results of configurations similar to the one under consideration. For example, the energy E_a of that illustrated in Fig. 4 is of relevance to the consideration of the shear modulus of the grain-boundary state. It can be computed with the following mathematical identities:

$$\sum_{n=-\infty}^{\infty} \frac{z^2}{(b+n)^2 + z^2} = \pi z \tan(\pi z) \frac{1 + \tan^2(\pi b)}{\tan^2(\pi b) + \tan^2(\pi z)}, \quad (\text{A9})$$

$$\sum_{\substack{n \neq 0 \\ n = -\infty}}^{\infty} \ln \frac{(n+b)^2 + z^2}{n^2} = \ln[\cosh(2z) - \cos(2\pi b)] - \ln(z^2 + b^2) - \ln(2\pi^2). \quad (\text{A10})$$

For z and b expressed in units of s , we obtain

perpendicular to the grain boundary as is illustrated in Fig. 3. This can be easily computed as follows. Note that first of all the contribution from V_1 is straightforward and one gets the same result as for $\theta=0$. The contribution from V_2 is given by

$$\bar{U}_2 = + \frac{K}{4\pi} \left[N \sum_n [\cos^2(\theta + \theta_n)] - (N-1) \sin^2 \theta \right].$$

The second term in the bracket comes from interactions between dislocations on the same grain boundary. \bar{U}_2 can be rewritten as

$$\frac{\bar{U}_2}{N} = + \frac{K}{4\pi} \left[\sum_n (\cos^2\theta \cos^2\theta_n - 2 \sin\theta \cos\theta \sin\theta_n \cos\theta_n + \sin^2\theta \sin^2\theta_n) + N(-1)\sin^2\theta \right].$$

Noting that $\sum_n \sin(2\theta_n) = 0$, we obtain

$$\begin{aligned} \bar{U}_2/N &= \left[\cos^2\theta \sum_n \cos^2\theta_n + \sin^2\theta \sum_n (2 - \cos^2\theta_n) - \sin^2\theta \right] K/4\pi \\ &= [(\cos^2\theta)\pi z/s \coth(\pi z/s) + (2N-1)\sin^2\theta] K/4\pi. \end{aligned} \quad (\text{A14})$$

This energy is smallest when $\theta=0$.

(4) Let us next consider the elastic energy of the grain boundaries, which is useful for finite-temperature considerations. A dislocation can interact with other dislocations on the same grain boundary or on another grain boundary. Let us denote these contributions by subscripts a and b . For transverse small deviations of the dislocations from their initial positions (see Fig. 5) we find that the change in the potential consists of contributions which are proportional to δz and $(\delta z)^2$, respectively. The first is short range and just gives Eq. (A6). We get, from the logarithmic (V_1) and the dipole (V_2) terms, the following:

$$\begin{aligned} \delta V_{2a} &= + \frac{K}{4\pi} \sum \frac{(\delta z_{i,n+m} - z_{i,m})^2}{n^2 s^2}, \\ \delta V_{1a} &= \frac{-K}{8\pi} \sum_{n=-\infty}^{\infty} \sum_{m=-\infty}^{\infty} \sum_{i \neq 0} \frac{1}{n^2 s^2} (\delta z_{i,n+m} - \delta z_{i,m})^2, \\ \delta V_b &= \frac{K}{4\pi} \sum_{i>j} \sum_{m=-\infty}^{\infty} \sum_{n=-\infty}^{\infty} \epsilon_i \epsilon_j \left[\frac{1}{2(z^2 + n^2 s^2)} - \frac{4z^2}{(z^2 + n^2 s^2)^2} + \frac{4z^3}{(z^2 + n^2 s^2)^3} (\delta z_{i,n+m} - \delta z_{j,m})^2 \right]. \end{aligned} \quad (\text{A15})$$

Here $\epsilon_i, \epsilon_j = \pm 1$.

Note that even though the dipolar term provides a zero contribution when δz is zero, it is responsible for the positive sign of δV_{2a} . Using the formulas

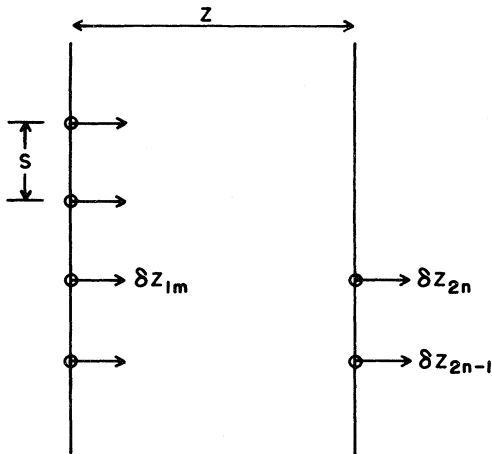


FIG. 5. Possible fluctuations of grain boundaries for normal model calculations.

$$\begin{aligned} \sum_n \frac{\cos(nks)}{n^2 + \alpha^2} &= \frac{\pi}{\alpha} \frac{\cosh[\alpha(\pi - s|k|)]}{\sinh(\alpha\pi)} \\ &\rightarrow \frac{\pi}{\alpha} - \pi|k|s + O(e^{-2\pi\alpha}), \\ \sum_n \frac{\cos(nks)}{(n^2 + \alpha^2)^2} &\rightarrow \frac{\pi}{2\alpha^3}, \end{aligned} \quad (\text{A16})$$

$$\begin{aligned} \sum_n \frac{\cos(nks)}{(n^2 + \alpha^2)^3} &\rightarrow \frac{3\pi}{\alpha^4}, \\ \sum_{n \neq 0} \frac{\cos(nks)}{n^2 s^2} &= \frac{\pi|k|}{s} - \frac{k^2}{2}. \end{aligned}$$

With $\delta z_{ik} = 1/\sqrt{N} \sum_j \exp(ik_j s) \delta z_{lj}$, we obtain

$$\begin{aligned} \delta V_b \rightarrow \frac{Kb^2}{4\pi} \sum_{i>j} \sum_k \epsilon_i \epsilon_j \left[\delta z_{ik} \delta z_{jk}^* \frac{\pi|k|}{s} \right. \\ \left. + (|\delta_{ik}|^2 + |\delta_{jk}|^2) \right. \\ \left. - 2\delta z_{ik} \delta z_{jk}^* \frac{s\pi}{z} \right]. \end{aligned} \quad (\text{A17})$$

Similarly

$$\delta V_a = \frac{K}{4\pi} b^2 \sum_i |\delta z_{ik}|^2 \left[-\frac{k^2}{2} + \frac{\pi k}{s} \right]. \quad (\text{A18})$$

When the sum over i, j is performed, the last term on the right-hand side of (A17) becomes

$$\left| \sum_i \sum_k \epsilon_i \delta z_{ik} \right|^2 s \pi / z.$$

It is nonzero only if the center of the positive and negative grain boundaries are separated. We shall assume that this is not so and ignore it from now on.

Combining the remaining terms, we get

$$\delta V_a + \delta V_b = \frac{Kb^2}{4\pi} \left[\sum_i |\delta z_{ik}|^2 \left[\frac{\pi |k|}{s} - \frac{k^2}{2} \right] + \sum_{i>j} \epsilon_i \epsilon_j \delta z_{jk}^* \delta z_{ik} \frac{\pi |k|}{s} \right]. \quad (\text{A19})$$

For small k , the k^2 term is negligible. The quadratic form (A19) can be diagonalized and we get $N-1$ modes of frequency $\gamma |k|$ and one mode of frequency $(2N+1)\gamma |k|$ where $\gamma = k/8s$. N here is the total number of grain boundaries. Let us illustrate this for the case $N=4$, the solution for general N is identical.

In that case, one is interested in the equation

$$\begin{vmatrix} 1-\lambda & \frac{1}{2} & -\frac{1}{2} & -\frac{1}{2} \\ \frac{1}{2} & 1-\lambda & -\frac{1}{2} & -\frac{1}{2} \\ -\frac{1}{2} & -\frac{1}{2} & 1-\lambda & \frac{1}{2} \\ -\frac{1}{2} & -\frac{1}{2} & \frac{1}{2} & 1-\lambda \end{vmatrix} = 0. \quad (\text{A20})$$

In writing this down we have expressed the eigenvalue in units of $\pi |k|/s$. The factors of $\frac{1}{2}$ come from the fact that $\sum_{i>j} = \frac{1}{2} \sum_{i \neq j}$. Adding rows 2, 3, and 4 to 1, we get

$$\left(\frac{1}{2}-\lambda\right) \begin{vmatrix} 1 & 1 & 1 & 1 \\ \frac{1}{2} & 1-\lambda & -\frac{1}{2} & -\frac{1}{2} \\ -\frac{1}{2} & -\frac{1}{2} & 1-\lambda & \frac{1}{2} \\ -\frac{1}{2} & -\frac{1}{2} & \frac{1}{2} & 1-\lambda \end{vmatrix} = 0. \quad (\text{A21})$$

Adding rows 2 and 3, we get

$$\left(\frac{1}{2}-\lambda\right)^2 \begin{vmatrix} 1 & 1 & 1 & 1 \\ 0 & 1 & 1 & 0 \\ -\frac{1}{2} & -\frac{1}{2} & 1-\lambda & \frac{1}{2} \\ -\frac{1}{2} & -\frac{1}{2} & \frac{1}{2} & 1-\lambda \end{vmatrix} = 0. \quad (\text{A22})$$

Subtracting rows 3 and 4, we get

$$\left(\frac{1}{2}-\lambda\right)^3 \begin{vmatrix} 1 & 1 & 1 & 1 \\ 0 & 1 & 1 & 0 \\ -\frac{1}{2} & -\frac{1}{2} & -1 & \frac{1}{2} \\ 0 & 1 & 1 & -1 \end{vmatrix} = 0. \quad (\text{A23})$$

Adding $\frac{1}{2}$ of row 1 to row 3, we get

$$\begin{vmatrix} 1 & 1 & 1 & 1 \\ 0 & 1 & 1 & 0 \\ 0 & 0 & \frac{3-2\lambda}{2} & 1 \\ 0 & 0 & 1 & -1 \end{vmatrix} \left(\frac{1}{2}-\lambda\right)^3 = 0,$$

and from this

$$\left(\frac{1}{2}-\lambda\right)^3 \left(\frac{5}{2}-\lambda\right) = 0. \quad (\text{A24})$$

It is not difficult to generalize this to the case of arbitrary N .

Let us next turn our attention to the longitudinal modes. δV_{2a} is of the same functional as Eq. (A15). δV_b is now given by

$$\delta V_b = \sum \frac{1}{2(z^2+n^2s^2)} + \frac{2z^2}{(z^2+n^2s^2)^2} - \frac{4z^4}{(z^2+n^2s^2)^3} (\Delta\delta\gamma)^2. \quad (\text{A25})$$

At small distances, using Eq. (A4) we get

$$\delta V_{2b} = \text{csch}^2(\pi\alpha)/4s^2.$$

This is the gap quoted in Eq. (7). Carrying out the same algebra as the previous calculation, we get the same final result for large distances for the transverse modes as for the longitudinal modes.

(5) Let us next discuss the elastic energy of Fig. 2(b). This is facilitated by using a Fourier series expansion for the dislocation density ρ . We shall only look at the limit $z/s \rightarrow \infty$ here. We have

$$\rho = \left[\sum_m A_m \exp(-2i\pi x m/l) + \frac{1}{3}\rho_0 \right] \delta(z),$$

$$A_m = (\rho_0/2\pi m) \sin(\pi m/3),$$

$$\rho_0 = \frac{1}{s}.$$

Note that ρ can be written as

$$\rho = \left[\sum_{m>0} 2A_m \cos(2\pi x m/l) + \frac{1}{3}\rho_0 \right] \delta(z).$$

The contribution from V_1 (called ϕ_1) can be computed from the equation $\nabla^2 \phi_1 = 2\pi\rho$ in two dimensions. Writing ϕ_1 as

$$\phi_1 = \sum_{m>0} \phi_{1m} \cos \left[\frac{2\pi x m}{l} \right] \exp \left[-\frac{2\pi m |z|}{l} \right] + \phi_0, \quad (\text{A26})$$

we find that

$$\frac{\delta\phi}{\delta z} = + \sum_{m>0} \text{sgn}(z) \frac{2\pi m}{l} \cos \left[\frac{2\pi x m}{l} \right] \times \exp \left[-\frac{2\pi |z|}{l} \right].$$

Since $\text{sgn}'(z) = +2\delta(z)$ we get

$$2 \frac{2\pi m}{l} \phi_{1m} = 2\pi(2A_m), \quad (\text{A27})$$

$$\phi_{1m} = \frac{A_m l}{m}.$$

Similarly, we get $\phi_0 = \pi\rho_0 z$. The contribution from V_2 (called ϕ_2) is most easily obtained by direct integration. One has

$$\begin{aligned} \phi_2 &= \sum_m A_m \exp \left[\frac{i2\pi m x}{l} \right] \int du \frac{z^2}{z^2 + u^2} e^{i2\pi m u/l} \\ &= \sum_{m>0} 2A_m \cos \left[\frac{2\pi m x}{l} \right] \pi |z| e^{-2\pi m |z|/l} + \pi\rho_0 z. \end{aligned} \quad (\text{A28})$$

Collecting terms we get

$$\begin{aligned} \phi &= \phi_1 - \phi_2 \\ &= \sum_{m>0} \cos \left[\frac{2\pi m x}{l} \right] \exp \left[\frac{2\pi m |z|}{l} \right] \\ &\quad + 2A_m \left[\pi |z| - \frac{l}{2m} \right]. \end{aligned} \quad (\text{A29})$$

The energy of Fig. 2(b) consists of interactions from dislocations on the same grain boundary (self-energy) as well as that from different grain boundaries. The self-energy E_1 is given by

$$\begin{aligned} E_1 &= \frac{-K}{4\pi} \int \phi(z=0, x) \rho(x) dx \\ &= -\frac{K}{4\pi} \sum_m (2A_m)^2 \left[\frac{-l}{2m} \right] \frac{l}{2} N \\ &= +\frac{K}{4\pi} \sum_m A_m^2 \frac{l^2}{m} N. \end{aligned} \quad (\text{A30})$$

The interaction energy per grain boundary E_2 is given by

$$\begin{aligned} E_2 &= \frac{K}{4\pi} \int \phi \left[z = \frac{\sqrt{3}l}{2}, x \right] \rho \left[x - \frac{l}{2} \right] dx \\ &= \frac{K}{4\pi} \sum_{m>0} (2A_m) \exp \left[-\sqrt{3}\pi m \left[\pi \frac{l\sqrt{3}}{2} - \frac{l}{2} \right] \right] (2A_m) \frac{l}{2N} \cos(\pi m) \\ &= \frac{K}{4\pi} \sum_{m>0} 4A_m^2 \cos(\pi m) \exp \left[-\sqrt{2}\pi m \left[\frac{\pi l\sqrt{3}}{2} - \frac{l}{2} \right] \right] \frac{l}{2} N. \end{aligned} \quad (\text{A31})$$

Combining we get for the total energy E ,

$$\begin{aligned} E &= \frac{K}{4\pi} \sum_{m>0} \frac{l^2}{s^2} \left[\frac{1}{m} + \cos(\pi m) \exp[-\sqrt{3}\pi m(\pi\sqrt{3}-1)] \right] \frac{\sin^2(\pi m/3)}{(2\pi m)^2} \\ &\cong \frac{K}{4\pi} \frac{\sin^2(\pi/3)}{(2\pi)^2} \{1 - \exp[-\sqrt{3}\pi(\pi\sqrt{3}-1)]\} \frac{Nl^2}{s^2} \\ &\simeq \frac{K}{64\pi^3} \frac{l^2}{s^2} N. \end{aligned} \quad (\text{A32})$$

APPENDIX B

(1) First let us record the calculation of the free energy of a single grain boundary. This calculation is trivial; however, since some numerical errors were made in a previous publication we shall write down some details here. The total free energy of an isolated grain boundary consists of two parts. First, there

is the elastic energy at zero temperature. From Eq. (A7), this is

$$F_1 = 2T_0 [\ln s - \ln(2\pi)] L/s. \quad (\text{B1})$$

I note that the energy in (A7) is that for a pair of grain boundaries. Recall also that $T_0 = K/16\pi$.

Next, there is the contribution from finite-

temperature entropy effects. This is determined from the equation

$$\exp[-(\beta F_2/2)] = \left[\int \prod_q du_q \exp(-\beta\gamma|q|u_q^2) \right]. \quad (\text{B2})$$

Note that there are contributions from both the transverse and longitudinal modes. Hence $F_2/2$ appears on the left-hand side of (B2). γ is given in Eq. (8). The limit of q is from $-\pi/s$ to π/s . From (B2), we get

$$F_2 = \frac{L}{s} [-2 \ln s - 1 + \ln(2\pi)] T. \quad (\text{B3})$$

Combining (B1) and (B3) we get

$$\begin{aligned} F_1 + F_2 &= \frac{L}{s} [(2T_0 - 2T) \ln s - 1 - \ln(2\pi)] \\ &= \frac{L}{s} \left[(T_0 - T) - \frac{2.84}{2 \ln s} \right] \ln s. \end{aligned} \quad (\text{B4})$$

(2) Next we discuss the entanglement energy of grain boundaries. By this we mean the following. At finite temperatures the grain boundaries are no longer straight. Instead, they increase their entropy by meandering over all space. When two parallel grain boundaries are close together, due to their hard-core repulsion a certain amount of entropy is lost. If the elastic energy were proportional to q^2 , previous calculations using path-integral techniques suggest that the entanglement energy is proportional to n^3 . This same functional dependence can also be produced by the following physical argument.

The total entropy loss is proportional to how frequently two grain boundaries are close to each other. This is proportional to n^2 per grain boundary and can be estimated as follows. Suppose that two grain boundaries are close at a point z_0 (see Fig. 6) and at a further distance l they are close together again. Then the frequency that we want is inversely proportional to the mean value of l . As one moves from z_0 the mean-square lateral fluctuation $(\delta x)^2$ increases. l is just determined by $\langle [\delta x(l)]^2 \rangle = n^{-1}$,

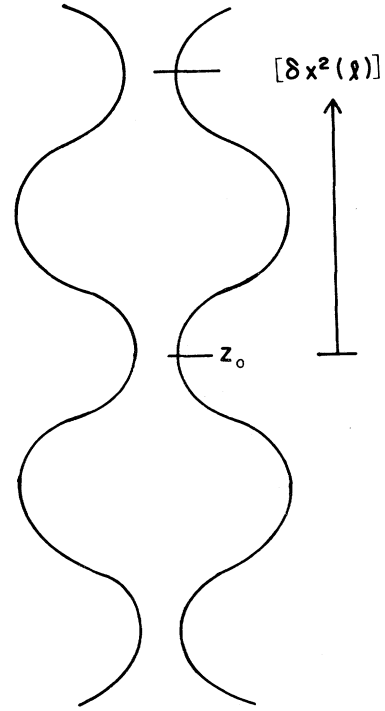


FIG. 6. Diagram illustrating the estimate of the fluctuation entropy of the grain boundaries.

the mean interboundary spacing. Since $[\delta x(l)]^2 \propto l$ we get $l^{-1} \propto n^2$. The total entropy lost per grain boundary is hence n^3 . This same argument has also been pointed out by Coopersmith *et al.*

Now that the elastic energy is proportional to $|q|$, the grain boundary is much stiffer. $[\delta x(l)]^2$ is given by the formula

$$[\delta x(l)]^2 = \int \frac{T}{\delta |q|} e^{iq l} dq \propto T \ln l. \quad (\text{B5})$$

By the same argument as above, the frequency at which two grain boundaries are close together is proportional to $\exp(-\text{const}/Tn^2)$. The total entropy lost is hence $n \exp(-\text{const}/Tn^2)$.

(3) Finally let us try to make an estimate of the grain-boundary crossing energy. The net gain in potential energy $\langle V \rangle$ is approximately given by

$$\langle V \rangle = \frac{1}{2} \left[- \frac{\int_A r dr (K/8\pi) \ln r e^{-\beta(K/8\pi) \ln r}}{\int_A e^{-\beta(K/8\pi) \ln r} r dr + \int_{A'} e^{-\beta(K/8\pi) \ln r} r dr} + \frac{\int_A (K/8\pi) \ln r e^{\beta(K/8\pi) \ln r} r dr}{\int_A e^{+\beta(K/8\pi) \ln r} r dr + \int_{A'} e^{+\beta(K/8\pi) \ln r} r dr} \right]. \quad (\text{B6})$$

Note that because the Burgers vectors are at an angle of 60° with respect to each other we have $K/8\pi$ and not $K/4\pi$ in the above expression. We have also neglected the angular terms [see Eq. (A13)] and have used the short-range part of the potential between a dislocation and a grain boundary. Since this range is of the order of s/π , we have approximated the region of integration A by

$$|r| < (2/\sqrt{3})s/\pi.$$

A' is the complement of A . The second term on the right-hand side of (B6) is much smaller than the first and hence is neglected. Carrying out the calculation, we get

$$\langle V \rangle \cong - \frac{\ln^2 s - \ln^2(\pi\sqrt{3}/2)}{(1 - 2/3\pi^2) + 2 \ln(2s/\pi\sqrt{3})} \frac{K}{16\pi}. \quad (\text{B7})$$

For $\ln(2s/\sqrt{3}\pi) \gg 0.5$, we have

$$\langle V \rangle \cong -[\ln s + \ln(\pi\sqrt{3}/2)]T_0/2. \quad (\text{B8})$$

APPENDIX C

The derivation of Eq. (18) from Eq. (17) will be described here. Focusing on the contribution of one bound dislocation pair, we have from Eq. (17),

$$e^{-\beta(\tilde{F} - \tilde{F}_0)} \cong (L^2/s) \int_1^{1/n} dx \int_1^{1/n} dx' \int_{-s/2}^{s/2} dy \int_{-\infty}^{\infty} dy' \exp\{-\beta[\bar{U}(r) - \bar{U}(r')]\} \\ \times [(x - x')^2 + (y - y')^2]^{-2} / \tilde{Z}, \quad (\text{C1})$$

$$\tilde{Z} \cong (L^2/s) \int_1^{n^{-1}} dx \int_1^{n^{-1}} dx' \int_{-s/2}^{s/2} dy \int_{-\infty}^{\infty} dy' [(x - x')^2 + (y - y')^2]^{-2}.$$

\bar{U} is the potential due to a grain boundary. We have included the discrete nature of the grain boundary so that for small r , \bar{U} contains an explicit dependence on y and differs from the potential U in Eq. (3). From Eq. (A13), $\bar{U}(r) \rightarrow (K/8\pi)\ln(x^2 + y^2)$ for $\pi r/s \ll 1$.

The origin of the coordinates in Eq. (C1) is one of the dislocations on a grain boundary. Hence we have the factor $(L/s) \int_{-s/2}^{s/2} dy$.

For large x , $\bar{U}(r)$ approaches a constant. For $x, x' \gg s/\pi$, the factor $\exp\{-\beta[\bar{U}(r) - \bar{U}(r')]\}$ is then equal to 1. We thus split the region of integration in Eq. (1) into four regions as follows:

$$\int_1^{1/n} dx \int_1^{1/n} dx' = \int_{s/2\pi}^{1/n} dx \int_{s/2\pi}^{1/n} dx' + \int_1^{s/2\pi} dx \int_1^{s/2\pi} dx' + \int_{s/2\pi}^{1/n} dx \int_1^{s/2\pi} dx' + \int_1^{s/2\pi} dx \int_{s/2\pi}^{1/n} dx'. \quad (\text{C2})$$

In the first two regions, we shall approximate the integral by replacing the factor $\exp\{-\beta[\bar{U}(r) - \bar{U}(r')]\}$ by 1. In the two remaining regions, we shall approximate $\bar{U}(r)$ by

$$\bar{U}(r) = \begin{cases} \frac{K}{4\pi} \left[\ln \sinh \left[\frac{x\pi}{s} \right] - \frac{\pi x}{s} \coth \left[\frac{\pi x}{s} \right] + \ln \left[\frac{s}{\pi} \right] \right], & x > s/2\pi \\ \frac{K}{8\pi} \ln(x^2 + y^2) - \frac{K}{4\pi} \frac{x^2}{x^2 + y^2}, & x < s/2\pi. \end{cases} \quad (\text{C3})$$

Substituting back into (C1) we get

$$\exp[-\beta(\tilde{F} - \tilde{F}_0)] \cong (B + C + A) / \tilde{Z}, \quad (\text{C4})$$

where $B, C(A)$ comes from the first (last) two regions of integration. \tilde{Z} can be evaluated using the formula

$$\int_{-\infty}^{\infty} dy' [(x - x')^2 + (y - y')^2]^{-2} = \pi / (2|x - x'|^3). \quad (\text{C5})$$

We get (with the cutoff included so that $|x' - x| \geq 1$),

$$\tilde{Z} = \frac{\pi}{2} \left[\frac{1}{n} - 2 + \frac{n}{1-n} \right] L^2 \\ \cong \frac{\pi}{2n} L^2 (1 + 2n - n^2). \quad (\text{C6})$$

The factor $2n$ in the parentheses comes from the hard core. Similarly, B can be evaluated. We get

$$\begin{aligned}
B &= \frac{\pi}{2} \frac{1}{n} \left[1 - \frac{ns}{2\pi} - n \frac{ns/\pi}{1 - ns/\pi} \right] L^2 \\
&\simeq \frac{\pi}{2} \left[\frac{1}{n} \left[1 - \frac{ns}{2\pi} \right] - \right] L^2 .
\end{aligned} \tag{C7}$$

The evaluation of A is more complicated. Using (C5) and (C3) we get

$$\begin{aligned}
A &\cong L^2 \frac{\pi}{2s} \int_1^{s/2\pi} dx \int_{s/2\pi}^{1/2n} dx' \int_{-s/2}^{s/2} dy \frac{e^{4x^2/(x^2+y^2)}}{(x^2+y^2)^2} \exp[-\beta U(r')] \frac{1}{|x'-x|^3} \\
&= \sum_{m=0}^{\infty} C_m L^2 \frac{\pi}{2s} \int_1^{s/2\pi} x^m dx \int_{-s/2}^{s/2} dy \frac{e^{4x^2/(x^2+y^2)}}{(x^2+y^2)^2} \int_{s/2\pi}^{1/n} dx' \frac{1}{(x')^{3m}} \exp[-\beta \bar{U}(r')] ,
\end{aligned} \tag{C8}$$

where

$$C_m = \frac{(+3)(+3+1) \cdots (+3+m)}{m!} . \tag{C9}$$

Using Eq. (C3), we find

$$\int_{s/2\pi}^{1/n} dx' \exp[-\beta \bar{U}(r')] (x')^{-m-3} = \left[\frac{\pi}{3} \right]^{m-2} \left[f(m) - \frac{(n^3/2\pi)^{2+m}}{16(2+m)} \right] , \tag{C10}$$

where

$$f(m) = \int_{1/2}^{\infty} \frac{du}{u^{3+m}} (\sinh u)^4 \exp(-4u) \coth u . \tag{C11}$$

Substituting back into (C9) we get

$$A \simeq \sum C_m L^2 \frac{\pi}{2s} \int_1^{s/2\pi} x^m dx \int_{-s/2}^{s/2} dy \frac{e^{4x^2/(x^2+y^2)}}{(x^2+y^2)^2} \left[\frac{\pi}{s} \right]^{m-2} \left[f(m) - \frac{(ns/2\pi)^{2+m}}{16(2+m)} \right] . \tag{C12}$$

The integral over y can then be done by expanding $\exp[4x^2/(x^2+y^2)]$ in an infinite series using the formula

$$\int_{-\infty}^{\infty} \frac{dy}{(x^2+y^2)^{2+n}} = \frac{\Gamma(m - \frac{1}{2})}{\Gamma(m)} \pi x^{-3-2n} . \tag{C13}$$

By direct numerical evaluation one finds that

$$\sum_{m=0}^{\infty} \frac{1}{m!} \frac{\Gamma(m - \frac{1}{2})}{\Gamma(m)} \cong 14.299 .$$

Substituting back into (C13) we get

$$\begin{aligned}
A &\cong \sum_m \left[mL^2 \frac{\pi}{2s} \right] \int_1^{s/2\pi} x^{m-3} dx (14.299\pi) \left[\frac{\pi}{s} \right]^{m-2} \left[f(m) - \frac{(ns/\pi)^{2+m}}{16(2+m)} \right] \\
&= (A_0 s + A_1 + A_2/s + \cdots) L^2 \frac{\pi}{2s} .
\end{aligned} \tag{C14}$$

Here A_0 comes from the $m=0$ term; A_1 , the $m \leq 1$ term; A_2 , $m > 1$ terms. A quick check indicates that the coefficients of this infinite series goes down like m^{-3} .

For $m=0$, the x integration is dominated by the small x contributions and the dominant contribution comes from the $\tan^{-1}(s/2x)$ term which we shall approximate by $\pi/2 - 2x/s$. We get

$$A_0 \cong \frac{\pi}{2} L^2 4\pi \left[f(0) - \frac{(ns)^2}{3 \times 2\pi^2} \right] \times 28.598 . \tag{C15}$$

Similarly we get

$$\begin{aligned}
A_1 &\cong C_1 \frac{\pi}{2} f(1) e^2 \cong \frac{3\pi}{2} e^2 f(1), \\
A_2 &\cong 28.598 \left[C_2 f(2) \frac{\pi}{2} \ln \left[\frac{s}{2\pi} \right] + C_3 \frac{f(3)}{4} - C_1 \pi f(1) - \pi C_0 \left[f(0) - \frac{(ns)^2}{32\pi^2} \right] \right].
\end{aligned} \tag{C16}$$

C can be evaluated approximately as

$$\left[\frac{1}{4} \right] \int_1^{s/2\pi} d^2 r' \int_1^{s/2\pi} d^2 r \left| \frac{r}{r'} \right| \frac{1}{|\vec{r} - \vec{r}'|^4} = \sum_m \int \int \left| \frac{r}{r'} \right|^4 \frac{r^m}{r^{4+m}} \int \text{Cm}^4[\cos(\Theta_1 - \Theta_2)] d\Theta_1 d\Theta_2,$$

where Cm^4 are the Gegenbauer polynomials.

The factor of $\frac{1}{4}$ comes about because we have been counting only one side of the grain boundary in calculating A , C , and Z whereas both sides are counted above. The above integral provides a lower bound for C since the region of integration in the above integral is actually smaller than the region of integration for C . It is not difficult to evaluate this integral. One gets

$$B = \frac{\pi}{2} \left[\frac{1}{8\pi} s^2 + O(s^0) \right]. \tag{C17}$$

Substituting (C6)–(C8) and (C15)–(C17) into (C4) we get

$$\begin{aligned}
\exp[-\beta(\tilde{F} - \tilde{F}_0)] &\cong 1 + ns \left[- \left[0.75 - f(0) \frac{14.299}{2} \right] / 2 - \left[1 + \frac{3e^2\pi}{2} f(1) \frac{1}{s} \right] \right] \\
&\quad + (ns)^2 \left[\frac{1}{4\pi^2} - \frac{1}{s} \frac{e^2 f(0)}{2\pi} - \frac{1}{s^2} \right] - \frac{e^2 (ns)^3}{128\pi^3}.
\end{aligned} \tag{C18}$$

$f(0)$ and $f(1)$ can be evaluated numerically on the computer. We found

$$f(0) = 0.0199,$$

$$f(1) = 0.01512,$$

and we get

$$\exp[-\beta(\tilde{F} - \tilde{F}_0)] \cong 1 + ns(-0.097 + 3.04/s) - 0.00186(ns)^2.$$

APPENDIX D

In Sec. V, we discuss the energy

$$H = \gamma \sum_q |q| |x_q|^2 + \lambda \sum_i \cos(2\pi x_i),$$

and claim that the calculation of its free energy can be mapped into that of a gas of 1D Coulomb rods and hence into the Kondo problem. This is done via essentially the same procedure as is carried out in the study of the roughening transitions.

Specifically, consider

$$\begin{aligned}
\exp(-\beta F) &= \int \prod_i dx_i \exp(-\beta H) \\
&= \sum \beta^n \lambda^n \int \left[\sum_j \sum_{\epsilon_j = \pm 1} \frac{1}{2} \exp(i 2\pi \epsilon_j x_j) \right]^n / n! \prod_i dx_i \left[\exp - \beta \gamma \sum_q |q| |x_q|^2 \right] \\
&= \sum_n \frac{(\beta \lambda / 2)^n}{n!} \sum_{\{\epsilon_j\}} \int \prod_j dx_j \exp \left[\sum_j 2\pi \epsilon_j x_j - \sum_q \beta \gamma |q| |x_q|^2 \right] \\
&= \sum_n \frac{(\beta \lambda / 2)^{2n}}{(2n)!} \sum_{\{\epsilon_j\}} \int \prod_q dx_q \exp \sum_q (2i\pi \epsilon_q x_q - \beta |q| \gamma |x_q|^2)
\end{aligned}$$

$$\begin{aligned}
&= \sum_n \frac{(\beta\lambda/2)^{2n}}{(2n)!} \sum_{\{\epsilon_j\}} \int \prod_q \left[\frac{\pi}{\beta|q|\gamma} \right]^{1/2} \exp \left[- \sum_q \frac{|2\pi\epsilon_q|^2}{4\beta|q|\gamma} \right] \\
&= e^{-\beta F_0} \sum_n \frac{(\beta\gamma/2)^{2n}}{(2n)!} \sum_{\{\epsilon_j\}} \exp \left[- \frac{\pi^2}{\beta\gamma} \sum_q \frac{|\epsilon_q|^2}{|q|} \right] \\
&= e^{-\beta F_0} \sum_n \frac{(\beta\lambda/2)^{2n}}{n!} \sum_{\{\epsilon_j\}} \exp \left[- \sum_{i,j} \epsilon_i \epsilon_j V(i,j) \right], \\
\exp -\beta F_0 &= \prod_q \left[\frac{\pi}{\beta\gamma|q|} \right]^{1/2}, \\
V(k,l) &= \frac{\pi^2}{\beta\gamma} \sum_q \frac{\exp[iq(k-l)]}{|q|} \frac{1}{N} \rightarrow \frac{\pi}{2\beta\gamma s} \ln \left[\frac{r}{s} \right].
\end{aligned}$$

From Eq. (8), we get

$$\pi/(2\beta_0\gamma s) = \frac{1}{4}.$$

From the literature for the Kondo problem, for a potential of the form $\sum_{i>j} \epsilon_i \epsilon_j \beta Q^2 \ln r_{ij}$, the phase transition occurs when $\beta Q^2 = 2$ in the limit of small λ . We expect the interface to roughen and the shear modulus will then be zero for $T > T_0/8$.

APPENDIX E

The question of the formation of the bound state will be discussed here. We argue that when a bound state is formed, a fraction of the two grain boundaries must be within a distance of s/π from each other. This portion of the grain boundaries gains a certain amount of energy at the expense of losing some entropy. For $T > T_0$, this is always unfavorable.

The loss in entropy comes from both the longitudinal and the transverse modes. For the longitudinal modes at close distances Δ in Eq. (7) is now finite so that the new free energy is

$$\bar{G}_1 = -T \frac{L}{S} \ln \left[\frac{\pi}{\beta\Delta} \right].$$

Comparing with Eq. (9), we get a difference $\Delta\bar{G}_1$ for the longitudinal modes given by

$$\Delta\bar{G}_1 = -T \frac{L}{S} \left[\ln \frac{\pi^2 z^2}{2s^2} - 1 \right].$$

Combining with Eq. (A6) we get an effective short-range potential U_{eff} given by

$$U_{\text{eff}} = (4T_0 - 2T) \ln(\pi z/s) + 0.466T_0.$$

For $z \gg s/\pi$, U_{eff} is zero.

The gain in free energy ΔF for any portion of the grain boundaries that are within a distance of s/π of each other is given by

$$\exp(-\beta\Delta F) = \int_1^{s/\pi} dz \exp[-\beta U_{\text{eff}}(z)].$$

From this, we get

$$\frac{s}{L} \Delta F = \left[-2 + \left[-\frac{T_0}{T} + 1 \right] \right] \ln \left[\frac{\pi}{s} \right] + 0.466T.$$

Comparing this with the entropy for the transverse modes [half of Eq. (9)] we get

$$-(4T_0 - 4T) \ln s + 3.6T_0.$$

Hence for $\ln s \leq 0.9/(T_0 - T)$ no bound state can form.

¹For rigid disks, see B. J. Alder, and T. E. Wainwright, Phys. Rev. **127**, 359 (1962). For inverse power potentials, see R. W. Hockney and T. R. Brown, J. Phys. C **8**, 1813 (1975); F. van Swol, L. V. Woodcock, and J. N. Cape, J. Chem. Phys. **73**, 913 (1980); R. H. Morf, Phys. Rev. Lett. **43**, 931 (1979); R. Kalia, P. Vashista, and S. W. de Leeuw, Phys. Rev. B **23**, 4794 (1981); J. Broughton, G. Gilmer, and J. D. Weeks, *ibid.* **25**, 4651 (1982). For Lennard-Jones potentials see D. Frenkel

and J. P. McTague, Phys. Rev. Lett. **42**, 1632 (1979); F. Abraham, *ibid.* **44**, 463 (1980); S. Toxvaerd, Phys. Rev. Lett. **44**, 1062 (1980). For Gaussian core potentials, see F. Stillinger and T. A. Weber, J. Chem. Phys. **74**, 4015 (1981).

²J. M. Kosterlitz and D. Thouless, J. Phys. C **6**, 1181 (1973).

³B. I. Halperin and D. Nelson, Phys. Rev. Lett. **41**, 121 (1978); D. Nelson and B. I. Halperin, Phys. Rev. B **19**,

- 2457 (1979).
- ⁴N. F. Mott and R. W. Gurney, *Trans. Faraday Soc.* 35, 364 (1939); S. Mizushima, *J. Phys. Soc. Jpn.* 15, 70 (1960); D. Kuhlmann-Wilsdorf, *Phys. Rev.* 140, 1599 (1965); F. R. N. Nabarro, *Theory of Crystal Dislocations* (Oxford University Press, Oxford, 1967); S. F. Edwards and M. Warner, *Philos. Mag. A* 40, 257 (1979).
- ⁵D. Fisher, B. Halperin, and R. Morf, *Phys. Rev. B* 20, 4692 (1979).
- ⁶W. T. Reed and W. Shockley, *Phys. Rev.* 78, 274 (1950).
- ⁷S. T. Chui, in *Melting, Localization, and Chaos*, edited by R. K. Kalia and P. Vashista (North-Holland, Amsterdam, 1982).
- ⁸S. T. Chui, *Phys. Rev. Lett.* 48, 933 (1982).
- ⁹P. G. de Gennes, *J. Chem. Phys.* 48, 2357 (1968). See also J. Villain, in *Ordering in Strongly Fluctuating Condensed Matter Systems*, edited by T. Riste (Plenum, New York, in press).
- ¹⁰See, for example, J. D. Weeks, *Phys. Rev. B* 24, 1530 (1981).
- ¹¹N. D. Mermin, *J. Math. Phys.* 8, 1061 (1967).
- ¹²See, for example, F. Stillinger and T. Weber (unpublished); Y. Saito, *Phys. Rev. Lett.* 48, 1114 (1982).
- ¹³P. A. Heiney, R. J. Birgeneau, G. S. Brown, P. M. Horn, D. E. Moncton, and P. W. Stephens, *Phys. Rev. Lett.* 48, 104 (1982).